Determination of the AlN nucleation layer thickness formed on the $Al_2O_3(0001)$ surface during nitridation process by XPS and IR spectroscopy

© D.S. Milakhin[1,2], T.V. Malin[1], V.G. Mansurov[1], A.S. Kozhukhov[1], N.N. Novikova[3], V.A. Yakovlev[3], K.S. Zhuravlev[1]

[1] Rzhanov Institute of Semiconductor Physics, Siberian Branch, Russian Academy of Sciences, 630090 Novosibirsk, Russia
[2] Novosibirsk State Technical University, 630073 Novosibirsk, Russia
[3] Institute of Spectroscopy, Russian Academy of Sciences, 108840 Troitsk, Moscow, Russia
E-mail: dmilakhin@isp.nsc.ru

Received March 2, 2022
Revised March 25, 2022
Accepted March 25, 2022

The effect of different degrees of the sapphire surface nitridation process completion on the AlN buffer layer morphology has been studied. It was found that $\sim$ 85% completion of the AlN crystalline phase formation promotes the growth of a two dimensional AlN buffer layer with a smooth surface morphology, regardless of the substrate temperature and ammonia flux. In contrast, during the AlN nucleation layer formation as a result of weak or excessive sapphire nitridation, a polycrystalline or three-dimensional AlN structures with a high density of inversion domains, respectively, were formed. Using independent methods of X-ray photoelectron spectroscopy and infrared spectroscopy of surface polaritons, the thickness of the AlN nucleation layer was determined at $\sim$ 85% degree of the nitridation process completion, which amounted to $\sim$ 1 monolayer.

Keywords: ammonia molecular beam epitaxy, AlN, sapphire, reflection high-energy electron diffraction, nitridation, inversion domains, X-ray photoelectron spectroscopy, surface polaritons.

DOI: 10.21883/SC.2022.08.54455.23

1. Introduction

After Isamu Akasaki [1], Hiroshi Amano [2] and Shuji Nakamura [3] have been successful in producing the first blue LED of high brightness based on the semiconductor compounds of the III-group elements and nitrogen (III-N) on the sapphire substrates (Al_2O_3), these semiconductors are regarded as a very promising group of materials for optical (the light-emitting diodes, the laser diodes and the UF photodetectors) and nanoelectronic applications. The year 2006 has seen an ultra-violet LED with the smallest wavelength (210 nm) based on AlN [4]. The large field, which also attracts the attention to the III-N, is microwave and power electronics due to perfect transport properties of the electrons, the presence of the piezoelectric effect and the phenomenon of spontaneous polarization in the III-N structures, including the high mobility of electrons ($\sim 1000\,\mathrm{cm^2\cdot V^{-1}\cdot s^{-1}}$ at 300 K for GaN), the high drift velocity ($\sim 2.7\cdot 10^7\,\mathrm{cm\cdot s^{-1}}$ at 300 K for GaN) and the high concentration of the two-dimensional electron gas $\sim 2\cdot 10^{13}\,\mathrm{cm^{-2}}$ (by an order higher than the concentration at the AlGaAs/GaAs heterointerface) in the Al(Ga)N/GaN heterojunction [5]. After the success in obtaining graphene, the AlN and GaN compounds have attracted research interest due to their producibility as ultra-thin layers with a graphene-like hexagonal structure [6–12] which can be used as a gate dielectric for insulating the two-dimensional conductors of the graphene or silicene type with a zero band gap in synthesizing the van der Waals crystals, thereby opening new perspectives in development of the nanoelectronics and spintronics [12].

Due to the optical transparency in the visible and UF wavelength ranges, the significant thermal conductivity ($38.5\,\mathrm{W\cdot m^{-1}\cdot K^{-1}}$ at 300 K), the thermal stability, the high crystal perfection and substantially lower cost in comparison with the SiC substrates and the nitride substrates, the sapphire is widely used as a material predominantly for optoelectronic applications, and it can also be used for tryout of the growth technology of heteroepitaxial structures for the transistors and ultra-thin layers with the graphene-like hexagonal structure. The processing complexities of the epitaxial growth of III-N on the Al_2O_3 substrate are correlated to large mismatch of lateral parameters of the crystal lattices and the coefficients of thermal expansion of growing layers of AlN/GaN and sapphire. In order to match the parameters of the crystal lattices of III-N and the substrate, the surface of Al_2O_3 is chemically transformed in the flux of active nitrogen, i.e. by nitridation, thereby forming a thin nucleation layer of the crystal AlN. The significance of the nitride layer formed as a result sapphire nitridation, for the

technique of formation of III-N was underlined in the studies of Kawakami [13], Rouvi'ere [14], Mohn [15], Stolyarchuk [16] et al.

The studies have shown that the rate of rate of the AlN nucleation layer formation depends on the nitridation conditions — the temperature of the substrate and the flux of active nitrogen. However, the data are different [17–20], and at the same time the kinetics of formation of the AlN crystalline phase is always the same [21]. Despite diverse studies of the process of nitridation and growth of the III-N subsequent layers by various authors, there are still unresolved issues — when it is necessary to finish the nitridation process and start the epitaxial growth of the AlN buffer layer, and what thickness of the AlN nucleation layer is for optimum nitridation of the sapphire surface.

The studies of the thin AlN nucleation layer forming on the sapphire surface require very sensitive methods. The X-ray photoelectron spectroscopy (XPS) provides limited information [20,22,23]. That is why the present study has applied the infrared (IR) reflection and the IR spectroscopy of surface polaritons (SP) as an independent tool to study the AlN films grown by the ammonia MBE on the sapphire substrates. The surface polaritons are a kind of nonradiative electromagnetic oscillations, which result from strong interaction of the electromagnetic waves (IR photons) with the optical phonons and propagate along the interface of the two media, if one of them is an absorbing one [24,25]. The SP electromagnetic field is concentrated near the AlN/sapphire heterointerface, thereby sensitizing this method to the presence of very thin layers (up to the nanosized ones) at the interfaces.

The present study has described the influence of nitridation process completion on the epitaxial growth of the AlN buffer layer and determined the thickness of the AlN nucleation layer in case of optimum nitridation of the sapphire surface by the XPS and IR spectroscopy of the surface polaritons, which amounted to ~ 1 monolayer.

2. Experimental procedure

The studied samples have been grown on the molecular beam epitaxy CBE-32(P) unit produced by Riber and adapted for ammonia MBE. The basic pressure in the chamber was $1.0 \cdot 10^{-9}$ Torr. The active nitrogen was sourced from high-purity ammonia (99.999%) in complex with additional purification Entegris filters designed to provide the degree of purification of the ammonia 99.999999%. The ammonia flux to the chamber was set by a flowrate Bronkhorst regulator designed to operate within the range $8-400$ sccm. The experiments were conducted by using the (0001) sapphire 2-inch substrates ready for epitaxy (the so called „epi-ready“ ones). Before the experiment, the sapphire substrates were subjected to the high-temperature annealing at the temperature of 900°C for 1 hour in the residual atmosphere at the pressure of $(2-5) \cdot 10^{-8}$ Torr in order to preliminarily purify the surface from residual carbon and hydrogen contaminants. The substrates were heated with absorption of heater radiation by a molybdenum layer of the 0.4-μm thickness, which was applied to an opposite side of the sapphire substrate. The heater was manufactured as a tantalum spiral put into a container made of the pyrolytic boron nitride. The luminance spectra of the heated substrates were recorded using a small-size diffraction instrument „Ocean Optics USB4000“, provided with a multi-channel silicon photodetector [26]. The initial roughness of the surface of the sapphire substrate used in the experiments was characterized by the root-mean-square deviation (RMS) of ~ 120 pm. The roughness was estimated by the atomic-force microscopy (AFM) from areas of $5 \times 5\,\mathrm{mkm}^2$. The sapphire surface has been nitridated at the substrate temperature of 840°C at the ammonia flowrate of 25 sccm during 35 minutes. The reflection high-energy electron diffraction (RHEED) used in the experiments is a unique *in situ* method of investigating a surface structure, reconstruction surface phase transitions and the kinetics of the surface chemical reactions. During exposure of the sapphire surface to the ammonia flux, the evolution of the general RHEED image was recorded by the analytical system kSA 400 with the high-resolution CCD camera with the high-sensitive optics specially designed for RHEED, and it also included the measurement of intensity of sapphire and AlN spots. The dependence of the intensity of the diffraction spot on time, which is reflected as the kinetic curves, allows studying the kinetics of the chemical reaction in the presence of crystalline phases. The process of plotting the kinetic curves is described in detail in the studies [21,27].

In order to evaluate the thickness of the AlN nucleation layer, the substrates were studied by XPS and IR spectroscopy of the surface polaritons. The method of attenuated total reflection (ATR) applies the effect of total internal reflection, which at larger angles of incidence results in an exponentially damped wave (of the near field), penetrating the sample for a depth of about one micron, at the prism border. By varying the incidence angles, it is possible to provide for match of the phase velocity of the damped wave and the SP phase velocity for effective transmission of the damped wave energy to the surface polaritons, which manifests itself in attenuation of the reflected intensity. The measurements of the ATR surface polaritons in the Otto configuration [24] and the measurements of the reflection spectra were performed using the infrared Fourier-spectrometer IFS66v (BRUKER). The ATR attachment with the KRS-5 prism (NPVO-1, produced by LOMO) was used at various angles of incidence ($20-60°$ in the prism) in the p-polarized light for investigating the transverse-magnetic (TM) surface polaritons. The lattice polarizer based on the KRS-5 substrate was used. The spectral resolution was $2\,\mathrm{cm}^{-1}$. The air gap between the prism and the sample (from several microns to dozens of microns) was regulated by polyethylene terephthalate ribbons or dust particles in the gap. The spectra of external reflection were measured at near-normal incidence of radiation in the

s-polarized light. The measured spectrum was compared with the calculated spectrum for the prism–gap–films–substrate structure. The permittivities of the films and the substrate were described using sets of damped harmonic oscillators. The software SCOUT-94 [28,29] varied the structure parameters and minimized the difference between the experiment and calculation spectra.

The present study has examined only surface polaritons at the frequencies $> 550\,\text{cm}^{-1}$, as only these SP branches can be in resonance with the AlN-film phonons.

The final stage has grown the AlN layer of the 1-μm thickness at the ammonia flowrate of 15 sccm at the substrate temperature of 940°C at the rate of $0.3\,\mu\text{m}\cdot\text{h}^{-1}$. The morphology of the produced AlN layers was studied by the atomic-force microscopy.

3. Experimental results

As a rule, when forming the AlN nucleation layer on the sapphire surface, the researchers make a reference to the nitridation time at the fixed substrate temperature and the fixed flowrate of active nitrogen [17–20]. However, the time of formation of the AlN nucleation layer may depend on the uncontrolled change of the background pressure in the growth station or high-energy electrons when using the RHEED method [27,30], thereby substantially reducing the reproducibility of the nitridation process. That is why it requires a universal criterion which takes into account the influence of all conditions (the substrate temperature, the ammonia flowrate, the nitridation time). This criterion is the completion of the nitridation process. To determine the completion of the nitridation process *in situ* one may refer to the intensity of the diffraction spot of the formed AlN crystalline phase on the kinetic curves using the RHEED method [20].

The experimental kinetic curve of the process of sapphire nitridation was taken to select several points (Fig. 1) to start the formation of the AlN buffer layer thereat. It has been shown that if starting the growth of the AlN buffer layer at the 100% completion of nitridation of the sapphire surface (it is suggested that in this case the formed AlN nucleation layer fully covers the sapphire) as corresponding to the point *3* on the kinetic curve, then the 3*D* AlN with a high density of the inversion domains, which is confirmed by the transmission diffraction pattern. If selecting, for the growth of the AlN buffer layer, the initial point *2*, which corresponds to the $\sim 85\%$ completion of formation of the AlN crystalline phase on the sapphire surface, then the AlN two-dimensional film with the smooth surface morphology and the metal polarity is formed, which is confirmed by the reflective diffraction pattern and the reconstruction (2×2). The epitaxial AlN growth in the point *1*, which corresponds to the nonnitridated/weakly nitridated surface of the sapphire is characterized by surface coarsening, thereby subsequently resulting in the growth of the polycrystal. It is important

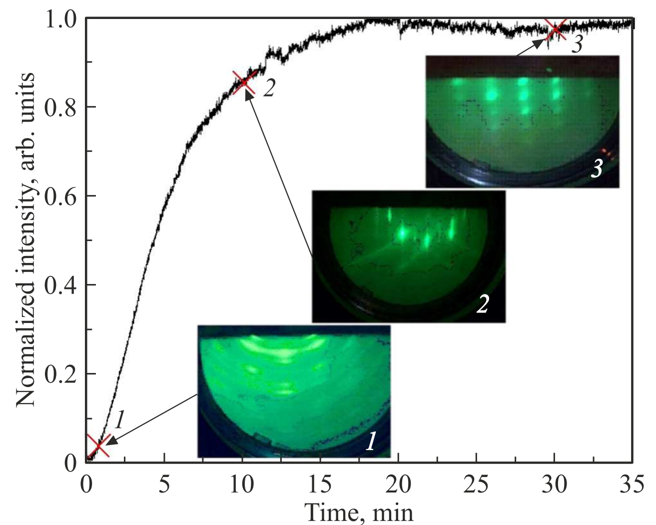

Figure 1. Kinetic curve of the nitridation process with the inserts of the diffraction patterns (DP) of the grown buffer layers (1 μm) at various completion of the nitridation (the points on the curve *1, 2* and *3*).

to note that the match of the points on the kinetic curve and the morphology of the surface of the AlN buffer layers will be maintained at any kinetic curves obtained at the various nitridation conditions, thereby underlining the universality of the completion criterion for the process of nitridation.

In order to study the completion of nitridation of Al_2O_3 on the surface morphology of the AlN buffer layer, the III-N structures have been grown on the initial (nonnitridated) sapphire substrate and the sapphire substrate nitridated at various stages of completion. Starting the growth of the AlN buffer layer at the point *3* of the kinetic curve of nitridation results in the structure with the high density of the inversion domains (Fig. 2, *a*). As a result, at the optimum stage of completion of nitridation (the point *2* on the kinetic curve), the AlN buffer layer without inversion domains has been obtained (Fig. 2, *b*). The AlN layers grown on the nonnitridated sapphire substrate or the point *1* of the kinetic curve of nitridation have a polycrystal structure (Fig. 2, *c*). It is suggested that the increase in the thickness of the nitridated layer results in the formation of a larger number of deflected AlN nuclei and the increase in the number of the inversion domains.

In order to obtain the information on the thickness of the nitridated layer for the $\sim 85\%$ completion of the nitridation process as corresponding to the point *2* of the kinetic curve of Fig. 1, the sample was studied by two independent methods of X-ray photoelectron spectroscopy and IR spectroscopy. The XPS method was used to record the change in the chemical composition of the surface of Al_2O_3 before nitridation and 10 minutes after at 840°C at the ammonia flowrate of 25 sccm. Fig. 3 shows the spectra of the initial and nitridated surfaces of the (0001) Al_2O_3

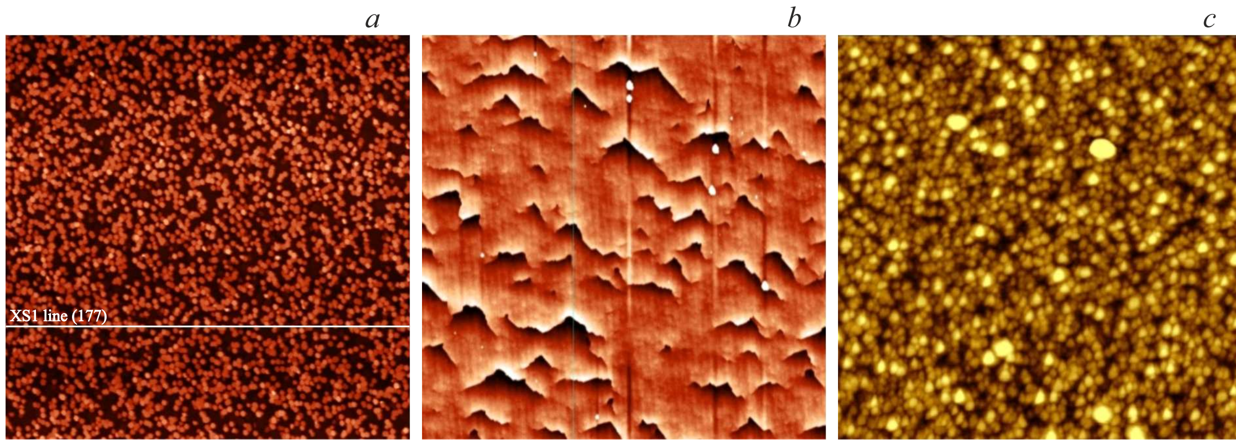

Figure 2. AFM-images of the $15 \times 15\,\text{mkm}^2$ grown AlN films ($1\,\mu$m) at the deeply-nitridated sapphire surface, which corresponds to the point *3* of the kinetic curve of nitridation (*a*), with the optimum ($\sim 85\%$) completion of the nitridation process at the point *2* of the kinetic curve (*b*) and on the nonnitridated substrate of sapphire or at the point *1* of the kinetic curve of nitridation (*c*). The *Z* height scale was, nm: *a* — 110, *b* — 10, *c* — 65. The height of the inversion domains on the film surface (*a*) was ~ 40 nm, the surface image (*b*) has no inverse domain, the surface roughness was ~ 0.5 nm.

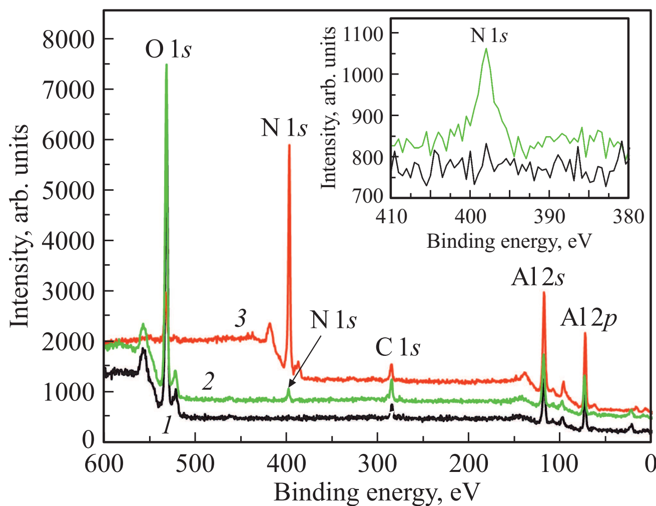

Figure 3. XPS-spectra of the samples: *1* — the initial surface of the (0001) Al_2O_3, *2* — the nitridated surface of the (0001) Al_2O_3, *3* — the surface of the (0001) AlN buffer layer. The insert shows the spectra of the initial and nitridated surface of the Al_2O_3 around the N1*s* peak.

and the surface of the (0001) AlN buffer layer. It is clear from the insert of Fig. 3 that the peak of the N1*s* nitrogen appears.

The thickness of the AlN nucleation layer synthesized as a result of nitridation has been calculated by the formula

$$I = I_0 \left(1 - e^{\left(-\frac{d}{\lambda}\right)}\right), \tag{1}$$

where I_0 — the calibration intensity of the N1*s* peak of the nitrogen atom in the AlN buffer layer, I — the intensity of the N1*s* peak of the nitrogen atom in the AlN nucleation layer on the Al_2O_3, d — the desired thickness of the AlN nucleation layer formed on the sapphire surface, λ — the typical depth of the electron output or, in other words, the average length of the free path of the electrons. The parameter λ was evaluated from the universal curve of the dependence of the free paths of the electrons λ on the kinetic energy E_{kin}. At $E_{\text{kin}} > 100$ eV, $\lambda \sim E_{\text{kin}}^{1/2}$. The kinetic energy of the electrons has been determined from the equation $E_{\text{kin}} = h\nu - E_{\text{bin}}$ to be equal to 1088.5 eV, where $h\nu$ — the energy of the exciting photon of the line Al $K\alpha$ 1486.6 eV, and E_{bin} — the binding energy of the emitted electron from the 1*s* level of the N atom, which is equal to 398.1 eV. In this case, the parameter λ is equal to ~ 33 Å. Thus, the calculation by the formula (1) shows that the thickness of the AlN nucleation layer synthesized as a result of nitridation is ~ 2 Å or ~ 1 monolayer (ML).

Fig. 4, *a* shows the external reflectivity (R) spectra initial and nitridated (at the point *2*) sapphire substrates, as well as of the AlN buffer layer grown on the sapphire substrate at the $\sim 85\%$ completion of formation of the AlN crystalline phase, at the near-normal incidence of radiation. It is clear from the graph that the R-reflection spectra of the initial and nitridated (at the point *2*) substrates are almost the same. The R-reflection spectrum of the AlN buffer layer considerably differs from the spectrum of the sapphire substrates due to light interference in the AlN film. The most important difference from the spectrum of the initial sapphire is an sharp maximum appearing at the frequency of $651\,\text{cm}^{-1}$ and marked by an arrow. This value corresponds to the perpendicular optical axis at the frequency of TO-phonon of the film (E-oscillations). Fig. 4, *b* shows the calculated spectral dependences of the imaginary parts of the permittivities for the studied AlN buffer layers (at the points *2* and *3*) and the substrates thereof.

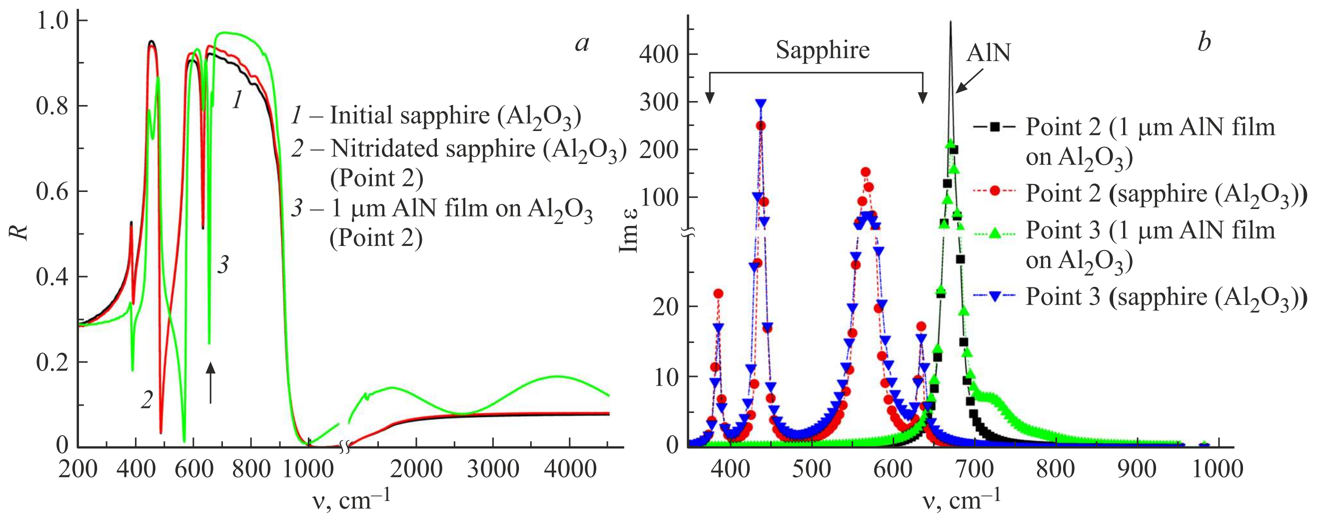

Figure 4. *a* — the experimental spectra of the external reflection at the near-normal incidence for the initial (*1*) and nitridated (*2*) sapphire substrate (at the point *2* on the kinetic curve), (*3*) for the AlN buffer layer (at the point *2*); *b* — the calculated imaginary part of the permittivity for the AlN buffer layer (at the points *2* and *3*). (A color version of the figure is provided in the online version of the article).

Figure 5. ATR-spectra of the initial (*a*) and nitridated (*b*) sapphire substrate (at the point *2*), as well as of the AlN buffer layer (*c*). The spectra are shifted along the ordinate axis. The radiation incidence angles are shown in degrees near the curves.

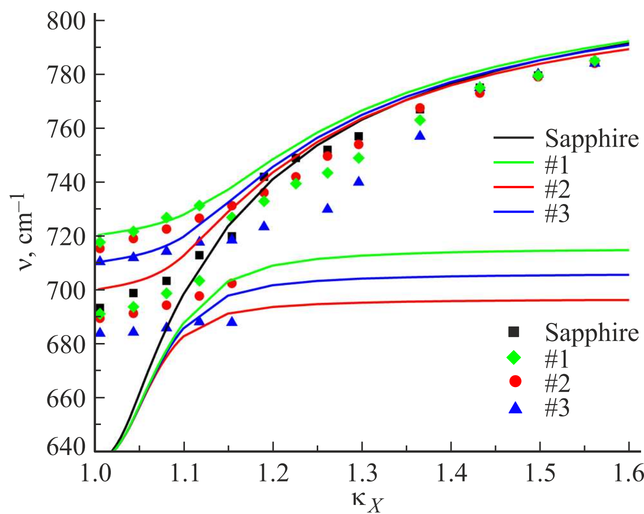

Figure 6. Dispersion curves for the initial (squares) sapphire sample and the three variously-nitridated sapphire samples: the point *1* — the rhombs, the point *2* — the circles, the point *3* — the triangles.

The peaks on the curves correspond to the frequencies of the TO-phonons of sapphire and AlN. It is clear from Fig. 4 that in order to obtain good approximation of the R-reflection spectrum for the sample formed at the $\sim 85\%$ completion of nitridation, it is necessary to take into account additional weak phonons with the frequencies of 682, 724, 784 cm^{-1}. It is suggested that these TO-phonons are originated from the transient area of the AlN layer formed near the sapphire substrate or caused by the presence of the N-polar sections of AlN.

The AlN nucleation layers formed as a result of exposure of the surface of the heated sapphire substrate to the ammonium flux were analyzed by the IR spectroscopy in the mode of attenuated total reflection. Since the SP electromagnetic field is concentrated near the AlN/sapphire interfaces, these excitations are more sensitive to a surface state or the presence of the very thin films in comparison with the external reflection method. Fig. 5 shows the ATR spectra of the initial and nitridated sapphire substrates (at the point *2*), as well as the AlN buffer layer (at the point *2*).

The minimum in the ATR spectra of the AlN buffer layer observed near the frequency of 800 cm^{-1} is caused by the surface polaritons available in the gap-AlN–sapphire structure. The comparison of the ATR spectra of the substrates of the initial and nitridated sapphire (at the point *2*) shows that the position of the minimum near the frequency of 700 cm^{-1} depends on the presence of the AlN crystalline phase on the sapphire surface. Some asymmetry of the minimum for the initial sapphire is caused by the angular width of the probing beam in the prism. Another minimum near the frequency of 630 cm^{-1} at these spectra is correlated to the sapphire substrate. The comparison of the ATR-spectra with the spectra generated using the model of damped harmonic oscillators demonstrates the presence of splitting of the minimums. The match of the transverse optical (TO) AlN frequency with the SP frequency results in a gap appearing in the SP dispersion curve due to the resonance interaction of sapphire SP with the TO-phonon of the AlN film. Fig. 6 shows the dispersion curves for the sapphire surfaces, as being initial and nitridated with the various completion (the points *1*, *2* and *3* on the kinetic curve). The symbols designate the positions of the minimums in the ATR spectra.

The position of the gap is determined by the frequency of the TO-phonon, which depends on the crystal structures, the atomic composition, deformation of the AlN, etc. The thickness of the AlN film is proportional to the square of the gap of the energy spectrum as per the formula

$$d = 2\Delta^2\lambda^3, \qquad (2)$$

where λ — the wavelength of the electromagnetic radiation ($\sim 10\,\mu$m). The thickness of the AlN nucleation layer as per this formula is ~ 0.25 nm or ~ 1 monolayer (ML), thereby correlating to the XPS-obtained results.

4. Conclusion

The present study has investigated the influence of the completion of the nitridation process on the growth of the AlN buffer layer. It is found that in formation of the AlN nucleation layer of the thickness of ~ 1 ML (the $\sim 85\%$ completion of the nitridation process on the kinetic curves) the AlN buffer layer will be subsequently grown without the inversion domains regardless of the nitridation conditions. This result allows substantially increasing the reproducibility of the subsequent III-N nanostructures. The RHEED, XPS, IR spectroscopy methods were used to investigate the initial and optimally nitridated sapphire as well as the AlN buffer layers of the 1-μm thickness grown as per the ammonia MBE method on the sapphire substrates. The high SP sensitivity allowed recording the change of the sapphire spectra after exposure of the surface to the ammonia flux, as well as when varying the nitridation time. It is found that the SP dispersion curves depend on a degree of transformation of the initial surface layer of sapphire to the crystalline AlN during nitridation. The surface morphology of the AlN buffer layers grown on the variously-nitridated sapphire substrate is different, thereby confirming the substantial influence of the nitridation process on the quality of the subsequent AlN films.

Funding

The study is financially supported by RF Ministry of Education and Science within the scholarship of the President of the Russian Federation to young scientists and graduate students for the years 2022–2024 the unique identifier is SP-1646.2022.3.

Acknowledgments

The AFM diagnostics was performed using the equipment of the Center of Shared Use „Technologies of nanostructuring, semiconductor, metal, carbon, bioorganic materials and analytical methods of their nano-level studies“ (CSU „Nanostructures“).

Conflict of interest

The authors declare that they have no conflict of interest.

References

[1] I. Akasaki. Rev. Mod. Phys., **87** (4), 1119 (2015). DOI: 10.1103/RevModPhys.87.1119
[2] H. Amano. Rev. Mod. Phys., **87** (4), 1133 (2015). DOI: 10.1103/RevModPhys.87.1133
[3] S. Nakamura. Rev. Mod. Phys., **87** (4), 1139 (2015). DOI: 10.1103/RevModPhys.87.1139
[4] Y. Taniyasu, M. Kasu, T. Makimoto. Nature, 441 (7091), 325 (2006). DOI: 10.1038/nature04760
[5] R.A. Ferreyra, C. Zhu, A. Teke, H. Morkoc. *Group III Nitrides*, ed. by S. Kasap, P. Capper (Springer International Publishing AG, 2017), Pt D (31), 743 (2017). DOI: 10.1007/978-3-319-48933-9
[6] C.L. Freeman, C. Frederik, L.A. Neil, H.H. John. Phys. Rev. Lett., **96** (6), 066102 (2006). DOI: 10.1103/PhysRevLett.96.066102
[7] H. Şahin, S. Cahangirov, M. Topsakal, E. Bekaroglu, E. Akturk, R.T. Senger, S. Ciraci. Phys. Rev. B, **80** (15), 155453 (2009). DOI: 10.1103/PhysRevB.80.155453
[8] A.L. Ivanovskiy. Uspekhi khimii, **81** (7), 571 (2012). [A.L. Ivanovskii. Russ. Chem. Rev., **81** (7), 571 (2012)] (in Russian). DOI: 10.1070/RC2012v081n07ABEH004302
[9] C.J.F. Solano, A. Costales, E. Francisco, A. Martín Pendas, M.A. Blanco, K.-C. Lau, H. He, R. Pandey. Comput. Model. Eng. Sci., **24** (2), 143 (2008).
[10] M. Houssa, G. Pourtois, V.V. Afanas'ev, A. Stesmans. Appl. Phys. Lett., **97** (11), 112106 (2010). DOI: 10.1063/1.3489937
[11] V. Mansurov, T. Malin, Yu. Galitsyn, K. Zhuravlev. J. Cryst. Growth, **428**, 93 (2015). DOI: 10.1016/j.jcrysgro.2015.07.030
[12] V.G. Mansurov, Yu.G. Galitsyn, T.V. Malin, S.A. Teys, K.S. Zhuravlev, I. Cora, B. Pecz. *2D Materials*, ed. by Ch. Wongchoosuk and Y. Seekaew (IntechOpen, 2018). DOI: 10.5772/intechopen.81775
[13] H. Kawakami, K. Sakurai, K. Tsubouchi, N. Mikoshiba. Jpn. J. Appl. Phys., **27** (2), L161 (1988). DOI: 10.1143/jjap.27.l161
[14] J.L. Rouviére, M. Arlery, R. Niebuhr, K.H. Bachem, O. Briot. Mater. Sci. Eng. B, **43** (1–3), 161 (1997). DOI: 10.1016/s0921-5107(96)01855-7
[15] S. Mohn, N. Stolyarchuk, T. Markurt, R. Kirste, M.P. Hoffmann, R. Collazo, A. Courville, R.D. Felice, Z. Sitar, P. Vennéguès, M. Albrecht. Phys. Rev. Appl., **5** (5), 054004 (2016). DOI: 10.1103/PhysRevApplied.5.054004
[16] N. Stolyarchuk, T. Markurt, A. Courville, K. March, O. Tottereau, P. Vennéguès, M. Albrecht. J. Appl. Phys., **122** (15), 155303 (2017). DOI: 10.1063/1.5008480
[17] K. Uchida, A. Watanabe, F. Yano, M. Kouguchi, T. Tanaka, S. Minagawa. J. Appl. Phys., **79** (7), 3487 (1996). DOI: 10.1063/1.361398
[18] N. Grandjean, J. Massies, M. Leroux. Appl. Phys. Lett., **69** (14), 2071 (1996). DOI: 10.1063/1.116883
[19] C. Heinlein, J. Grepstad. Appl. Phys. Lett., **71** (3), 341 (1997). DOI: 10.1063/1.119532
[20] F. Dwikusuma, T.F. Kuech. J. Appl. Phys., **94** (9), 5656 (2003). DOI: 10.1063/1.1618357
[21] D.S. Milakhin, T.V. Malin, V.G. Mansurov, Yu.G. Galitsyn, K.S. Zhuravlev. J. Therm. Anal. Calorim., **133** (11), 1099 (2018). DOI: 10.1007/s10973-018-7116-z
[22] K. Masu, Y. Nakamura, T. Yamazaki, T. Shibata, M. Takahashi, K. Tsubouchi. Jpn. J. Appl. Phys., **34** (6B), L760 (1995). DOI: 10.1143/JJAP.34.L760
[23] Y. Cho, Y. Kim, E. R. Weber, S. Ruvimov, Z.L. Weber. J. Appl. Phys., **85**, 7909 (1999). DOI: 10.1063/1.370606
[24] V.M. Agranovich, D.L. Mills (eds). *Surface Polaritons* (North-Holland Publ. Co., Amsterdam, 1982).
[25] G.N. Zhizhin, M.A. Moskaleva, E.A. Vinogradov, V.A. Yakovlev. Appl. Spectrosc. Rev., **18**, 171 (1982).
[26] T.V. Malin, V.G. Mansurov, A.M. Gilinskii, D.Yu. Protasov, A.S. Kozhukhov, A.P. Vasilenko, K.S. Zhuravlev. Optoelectron. Instrument. Proc., **49**, 429 (2013). DOI: 10.3103/S8756699013050026
[27] D.S. Milakhin, T.V. Malin, V.G. Mansurov, Yu.G. Galitsyn, A.S. Kozhukhov, D.E. Utkin, K.S. Zhuravlev. Appl. Surf. Sci., **541**, 148548 (2021). DOI: 10.1016/j.apsusc.2020.148548
[28] W. Theiß. The SCOUT through CAOS, Manual of the Windows application SCOUT.
[29] W. Theiß. Surf. Sci. Rep., **29**, 91 (1997).
[30] D.S. Milakhin, T.V. Malin, V.G. Mansurov, Yu.G. Galitsyn, K.S. Zhuravlev. Phys. Status Solidi B, **256**, 1800516 (2019). DOI: 10.1002/pssb.201800516